ELSEVIER

Journal of Power Sources 58 (1996) 221–224

JOURNAL OF POWER SOURCES

Short Communication

Vanadium–manganese complex oxides as cathode materials for aqueous solution secondary batteries

H.Q. Yang, D.P. Li, S. Han, N. Li, B.X. Lin

Department of Chemistry, Peking University, Beijing 100871, People's Republic of China

Received 19 October 1995; revised 10 January 1996

Abstract

Vanadium–manganese complex oxides are synthesized by heating NH_4VO_3 and $MnCO_3$ under various V:Mn mole ratios, different temperatures and atmospheres. The complex oxides are evaluated as cathode materials for aqueous solution secondary batteries.

Keywords: Vanadium oxide; Cathodes; Secondary materials; Manganese oxide

1. Introduction

Many studies have focused on secondary non-aqueous lithium batteries that use vanadium oxide as a cathode because of their high energy densities and good cycling lives [1–3]. In previous work, we have prepared V_2O_5–MnO_2 mixed oxides by heating NH_4VO_3 and MnO_2 under various conditions. The products with V:Mn = 1:1 mole ratio, obtained at 350 °C for 8 h in air, displayed the highest specific capacity and good cycling characteristics. In the present paper, V–Mn complex oxides are prepared using NH_4VO_3 and $MnCO_3$ as starting materials. The synthetic products are characterized by X-ray diffraction analysis, infrared spectroscopy and scanning electron microscopy. The relationship of synthetic conditions, structure and electrochemical performance of the samples are investigated for secondary aqueous solution batteries. The mechanism of Li^+ intercalation and de-intercalation and the framework of the composites are also discussed.

2. Experimental

V–Mn complex oxides were prepared by heating NH_4VO_3 and $MnCO_3$ (Beijing Chemical Factory) under various conditions, including different V:Mn mole ratios, temperatures, times and atmospheres. The composites were combined with graphite and polytetrafluoroethylene (PTFE) powder in a weight ratio of 2:10:1 and pressed on a nickel mesh (under 20 MPa for 1 min) to serve as cathodes for electrochemical cells. The dimensions of the cathode are 2.3 cm × 2.3 cm. A zinc foil was used as the anode, and saturated LiOH aqueous solution (saturated with ZnO) as the electrolyte. The charging/discharging behaviour of the cells was observed at 2 mA cm^{-2} and 25 °C. The powder obtained from different preparation conditions and the cathode products after charge/discharge cycles were analysed by X-ray diffraction analysis (XRD), infrared analysis (IR) and scanning electron microscopy (SEM) using a Rigaku D/Max-rA diffractometer with Cu Kα radiation, a Nicolet 5-Mx IR spectrometer (KBr pellet) and a KYKY-1000 microscope, respectively.

3. Results and discussion

3.1. Influence of V:Mn mole ratio

The SEM micrographs of the products synthesized under various conditions are shown in Fig. 1. The XRD patterns of the products obtained from heating mixtures of NH_4VO_3 and $MnCO_3$ with different V:Mn mole ratios at 350 °C for 4 h are presented in Fig. 2. The products consisted mainly of V_2O_5 and β-MnO_2. Mn_2O_3 and/or $Mn_2V_2O_7$ peaks appeared in each sample, except for that with a V:Mn = 0.6:1 mole ratio (sample D-6). Only one peak of β-MnO_2 appeared in the spectrum of D-6 at $2\theta = 36.4°$. A comparison was made of the 2θ values for the nine V_2O_5 peaks in Fig. 2(a) and (c). The 200, 001, 101 peaks of D-6 sample deviate to a smaller degree, while the 110, 400, 011, 310, 600 and 020 peaks deviate to a larger degree than the V_2O_5 sample. These results strongly suggest that Mn atoms have entered the lattice of

PII S0378-7753(96)02380-1

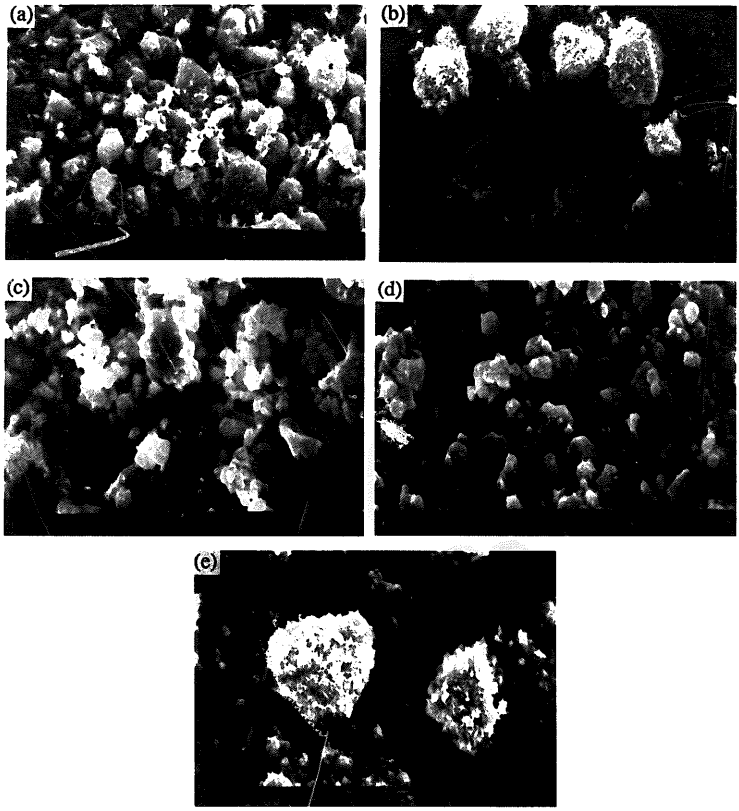

Fig. 1. SEM micrographs of products synthesized under different conditions: (a) V_2O_5 (NH_4VO_3; 350 °C; 8 h in air); (b) NH_4VO_3:MnO_2 = 1:1 (mole); 350 °C; 8 h in air; (c) NH_4VO_3:MnO_2 = 1:1 (mole); 500 °C; 8 h in air; (d) NH_4VO_3:$MnCO_3$ = 0.6:1 (mole); 350 °C; 4 h in air; (e) NH_4VO_3:$MnCO_3$ = 1:1 (mole); 350 °C; 16 h in air.

V_2O_5 during baking and that the layer structure of V_2O_5 has distorted.

The IR spectra of V_2O_5 (from decomposition of NH_4VO_3) and the D-6 sample are given in Fig. 3. The IR spectrum of D-6 is different from that of V_2O_5, namely, Mn–O band adsorbing peaks appear at 862 and 715 cm^{-1}, while the δ_{V-O} peak disappears at 480 cm^{-1} and other peaks of V–O bonds shift slightly towards higher wave numbers. These differences are probably caused by Mn entering into the lattice of V_2O_5 to form V–Mn complex oxides.

Typical discharge curves of an electrochemical cell using the V–Mn complex oxide as the cathode (D-6) at 2 mA cm^{-2} in saturated LiOH aqueous solution are presented in Fig. 4. The change in specific capacity with V:Mn mole ratio is given in Fig. 5. The specific capacity versus cycle number for the electrochemical cells is shown in Fig. 6. The D-6 sample gives the highest capacity and the best cycling characteristics.

3.2. *Influence of atmosphere*

The XRD pattern of product D-6 formed under an O_2 atmosphere is shown in Fig. 7. The O_2 sample has more Mn_2O_3 and $Mn_2V_2O_7$ peaks than the sample prepared in air. A comparison of the specific capacities of both samples is presented in Fig. 8. The results show that the electrochemical performance is poor for the O_2 sample.

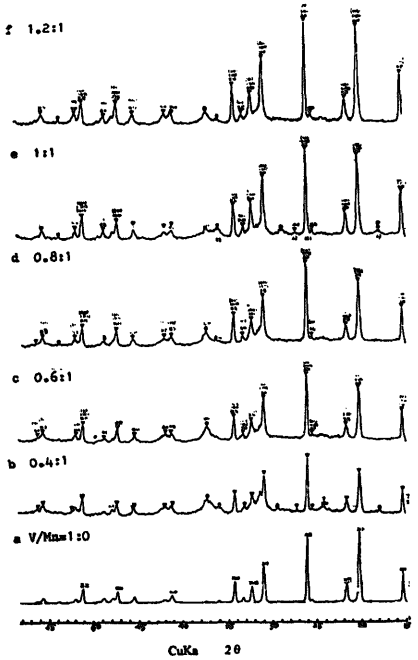

Fig. 2. XRD patterns of V–Mn complex oxides with different V:Mn mole ratios, at 350 °C for 4 h in air.

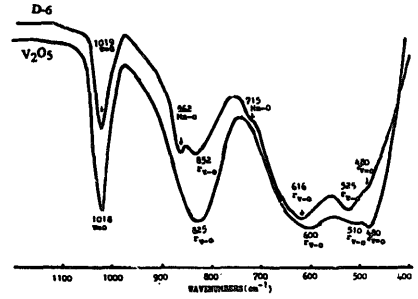

Fig. 3. IR spectra of V_2O_5 and D-6 sample.

3.3. Mechanism of Li^+ intercalation/de-intercalation into V–Mn complex oxide

The XRD patterns and IR spectra of the cathode product after different cycles are given in Figs. 9 and 10, respectively. In Fig. 9, the $LiMn_2O_4$ characteristic peaks at $2\theta = 18.5°$ and 36.5° are observed, but all of the peaks for V_2O_5 have disappeared. In Fig. 10, the D-6 sample is remarkable in that the V=O (1020 cm^{-1}) and V–O (825 cm^{-1}) peaks have dis-

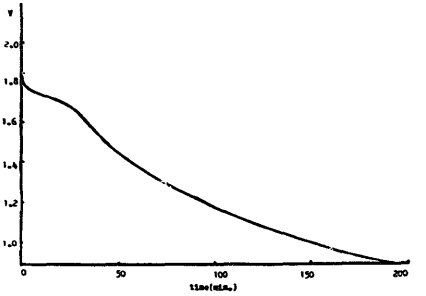

Fig. 4. Typical discharge curves of the cell at 2 mA cm^{-2}.

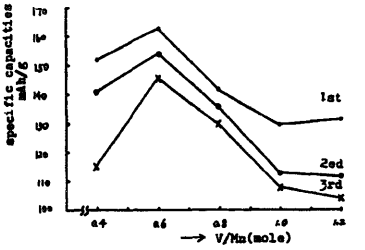

Fig. 5. Specific capacities of cathode composites with different V:Mn ratios.

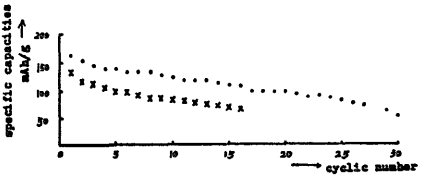

Fig. 6. Specific capacity vs. cycle number. (×) NH_4VO_3:MnO_2 = 1:1 (mole), 350 °C, 8 h in air; (●) NH_4VO_3:$MnCO_3$ = 0.6:1 (mole), 350 °C, 4 h in air.

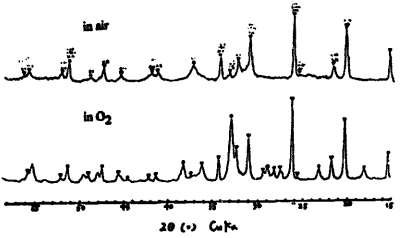

Fig. 7. XRD patterns sample D-6 in O_2 and in air.

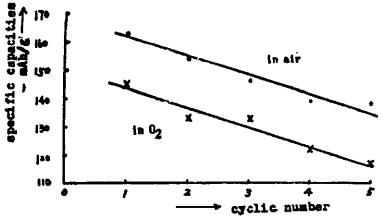

Fig. 8. Specific capacities of the cell using D-6 as cathode, formed in different atmospheres.

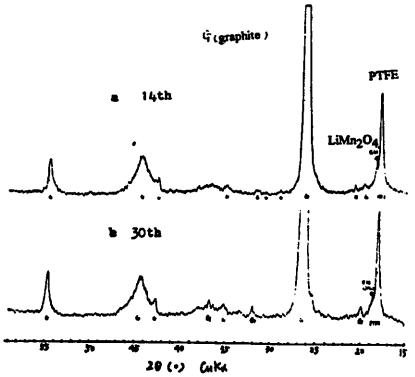

Fig. 9. XRD pattern of cathode products after different cycles.

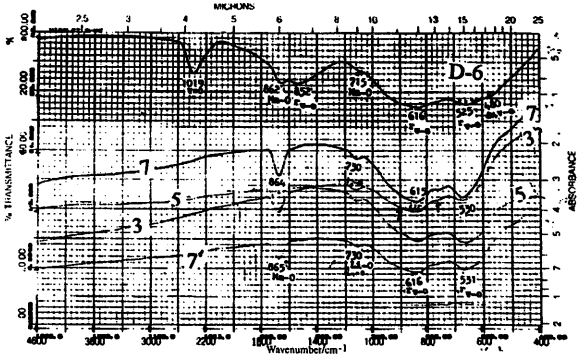

Fig. 10. IR spectra of cathode products after different cycles. 3, 5, 7 relate to discharge cycle number; 7′ relates to 7th charge.

appeared and the Li–O absorbing peak appears at 730 cm^{-1}. In addition, the γ_{V-O} (620 and 530 cm^{-1}) peaks have moved slightly to smaller wave numbers and the absorbing peaks become increasingly broader charge/discharge cycling. Inductively coupled plasma (ICP) analysis was performed for the electrolyte after the 30th cycle. There was only 0.48 mg V in 18 ml solution. This indicates that there is very little dissolution of the V–Mn complex oxide. The XRD, IR and ICP measurements give rise to the following conclusion. During discharging, Li^+ ions are inserted into the lattice of the composite and result in the formation of $LiMn_2O_4$. Meanwhile, some V–O bonds are broken and the crystal structure of V_2O_5 becomes amorphous.

4. Conclusions

The charge/discharge performance of V–Mn complex oxides formed by heating NH_4VO_3 and $MnCO_3$ (V:Mn = 0.6:1; 350 °C; 4 h in air) shows an initial specific capacity of up to 163 mAh/g cathode material. XRD, IR and ICP analyses prove that Mn enters the layer structure of V_2O_5 and distortion occurs. During discharging, Li^+ is inserted into the framework of the complex and Li–O bonds are formed. Concomitantly, some V–O bonds are broken and the crystal structure of V_2O_5 becomes amorphous. On further discharge, Li^+ is inserted in the crystal structure and results in the formation of $LiMn_2O_4$.

References

[1] J. Desilvestro and O. Haas, *J. Electrochem. Soc., 137* (1990) 5C.
[2] N. Kumagai, S. Tanifuji and Tanno, *J. Power Sources, 35* (1990) 313.
[3] N. Kumagai, S. Tanifuji, T. Fujiwara and K. Tanno, *Electrochim. Acta, 37* (1992) 1039.